Japanese Journal of Gastroenterology and Hepatology

Research Article

ISSN: 2435-1210 | Volume 10

Disassembly of Hepatitis B Virus Capsid Induced by Ellagic Acid

Wang P[1], Sun H[2], Liu Q[1,*]

[1]Department of Vegetables, College of Horticulture, China Agricultural University, Beijing 100193, China

[2]State Key Laboratory of Agrobiotechnology, China Agricultural University, Beijing 100193, China

***Corresponding author:**

Qinghong Liu,
Department of Vegetables, College of Horticulture,
China Agricultural University, Beijing 100193, China,
Tel: +86-10-62732578.

Received: 26 Feb 2024
Accepted: 06 Apr 2024
Published: 12 Apr 2024
J Short Name: JJGH

Keywords:

Hepatitis B virus; Ellagic Acid; Capsid Protein; Disassembly; Anti-HBV drug

Citation:

Liu Q. Disassembly of Hepatitis B Virus Capsid Induced by Ellagic Acid. J Gastro Hepato. 2024; V10(9): 1-8

1. Abstract

Ellagic acid (EA) reacted with hepatitis B virus (HBV) capsid core protein, induced the disassembly of HBV normal capsid *in vitro*. Both native agarose gel electrophoresis and TEM showed that EA treatments caused capsid disassembly. The disassembly mediated by EA led to formation of small heterogeneous aggregates which have dimer-like antigenicity. Docking analysis of EA and HBcAg predicted two putative binding sites, indicative of EA interaction with select amino acid residues, leading to a lack of stability of the global capsid structure. Ellagic acid might be one effective anti-HBV drug by blocking HBV production.

2. Introduction

Two billion people are reported to be infected with the hepatitis B virus (HBV), an enveloped DNA virus with an icosahedral capsid. Among those infected, more than 350 million have chronic HBV infections, and approximately 500,000-700,000 people die annually [1,2]. Chronic HBV infection causes cirrhosis, hepatocellular carcinoma and other serious health consequences [3-5]. Alpha interferon and polymerase inhibitors such as lamivudine and adefovir are approved treatments for chronic HBV [6,7]. With alpha interferon, a sustained response is kept in only a minority of cases and dose-limiting side effects disturbs clinical applications [8,9]. Contrastingly, treatment with nucleoside analogues usually lead to the development of drug resistant mutants [10-12]. All these observations call for a greater effort to diversify the therapeutic and prophylactic arsenal for HBV. Mature HBV virus particles consist of its genome and reverse transcriptase, encapsidated in a protein capsid composed of HBV core protein (Cp). Infectious DNA-containing particles are produced by reverse transcription solely within the intact core residing in the cytoplasm [13]. Therefore, a high value therapeutic approach to treat HBV infections may use targeted disruption of the capsid assembly process [14]. The prevalent form of the capsid is composed of 120 homodimers of Cp arranged with T=4 icosahedral symmetry [15-17]. The Cp assembly domain (Cp149) (residues 1-149) lacking the 34-residue C-terminal RNA-binding domain is usually used for Cp assembly studies [18-20]. The crystal structure of the T=4 capsid (Cp149) bacterially expressed has been solved by X-ray crystallography to 3.3 Å resolution [21]. Several small molecules that target the HBV core particle have been identified. Of these, Bis-ANS, a fluorescent probe, was found to be both a noncompetitive inhibitor and an assembly misdirector [22]. Heteroaryldihydropyrimidines (HAPs) were identified as a novel class of HBV drugs targeting the capsid. In particular, HAP antiviral compound Bay 41-4109 and its derivates could cause the formation of aberrant capsid [23,24]; HAP-1, a representative HAP compound, acting as an allosteric effector, accelerated the normal assembly of capsid at low concentration, while causing large-scale misdirection of assembly at higher concentrations [25]. Further researches focusing on small molecules that specifically disassemble the HBV core particle will enable identification of new therapeutic compounds. Herbs of the genus Phyllanthus have been used in the treatments of chronic hepatitis caused by HBV for a long time [26-28]. Lee et al. isolated ellagic acid (EA) from Phyllanthus urinaria, and demonstrated that EA effectively blocked the hepatitis B virus-e antigen secretion in HepG2.2.15 cells [29]. EA, that belongs to tannin family of water soluble phenolic compounds (Figure 1A), has been further shown to exhibit hepatoprotective activity by inhibition of liver fibrosis induced by CCl4 [30]. EA also was shown to inhibit host immune tolerance induced by HBeAg during HBV

infection [31], however the anti-HBV mechanism of EA remains a mystery. In earlier studies, drugs targeting the capsid were mainly classified as inhibitor and/or misdirector, based on their ability to inhibit and/or misdirect polymerization of capsid assembly process [22,25]. In this study we report a novel mechanism of EA inhibition of HBV that causes labilization followed by disassembly of the HBV mature core particle. The newly identified anti-HBV function of EA might aid in the discovery of novel antivirals that target the capsid.

3. Materials and Methods

3.1. Capsid Reconstitution and its Disassembly

Cp149 was expressed using a pET30a vector in E. coli expression system. Cp149 dimer was dissolved in a reaction buffer (20 mM phosphate buffer, 100 mM NaCl, pH 7.5) to assemble the core particle, and purified as previously described [32]. The resulting core particle solution at a concentration of 1.5 mg/ml was stored at −80 °C. Rabbits were injected with the protein and the polyclonal antibodies were purified from rabbit serum by protein A affinity chromatography (GE Healthcare, Uppsala, Sweden). The specificity of the polyclonal antiboby was detected towards both the subunit and capsid. EA (Sigma, St. Louis, MO) was dissolved in the same reaction buffer. To examine the effect of EA on the disassembly of mature capsid, ten-fold dilution of capsid stock were incubated with EA concentrations of 25, 100, 250 μg/ml at 26 °C for 12 h. To detect the time effect, disassembly reaction was performed at different reaction times (0 h, 3 h, 6 h, 9 h and 12 h).

3.2. Native Agarose Gel Electrophoresis

After disassembly reaction, HBV core particles were detected by native agarose gel electrophoresis as previously described [19,33]. Each sample was mixed with 6× loading buffer containing 0.25% bromophenol blue and 30% glycerol, and separated through 1% agarose in 40 mM Tris acetate and 1 mM EDTA. Alternatively, following electrophoresis, proteins in the gel were transferred onto nitrocellulose membrane (Pall, NY) at 200 mA for 4 h in 10× SSC, which was timesaving when compared with capillary transfer. HBV core particles on the membranes were analyzed by immunoblotting with the polyclonal antibody.

3.3. Transmission Electron Microscopy (TEM)

Samples after disassembly reaction were transferred to carbon-coated grids and stained with 1% uranyl acetate for 3 min. Samples were visualized on a JEM-1230 transmission electron microscope (JEOL, Tokyo, Japan) at a magnification of ×100 000. Images were collected by Morada camera (Soft Imaging System, Muenster, Germany) and analyzed by iTEM software.

3.4. Size Exclusion Chromatography (SEC)

The results of capsid disassembly reaction were detected by SEC on a 24 ml Superdex75 10/300 column mounted on an ÄKTA FPLC workstation (Amersham Biosciences, Uppsala, Sweden). The column was equilibrated with PBS at a flow rate of 0.5 ml/min. Samples (100 μl) were loaded by an auto injection module. The proteins were separated to two fractions, viz., capsid (7.0-8.3 ml) and small heterogeneous aggregates (10.3-17.0 ml). Protein peaks were quantified at 280 nm and analyzed by Unicorn 4.11 software. EA had no effect on A280 readings. The dissociation level was evaluated by counting

$$\text{Depolymerization coefficient} = \frac{\Delta S_2}{\Delta S_1}$$

ΔS_1 stands for the reduced peak area of capsid in the presence of EA, whereas ΔS_2 stands for the incremental peak area of small heterogeneous aggregates in the presence of EA. Fractions were collected and analyzed by ELISA assay.

3.5. Enzyme-Linked Immunosorbent Assay (ELISA)

Microtiter plates (Corning, NY) were coated with rabbit polyclonal anti-HBc Ab in 0.05 M sodium bicarbonate (pH 9.5) overnight at 4 °C and blocked with 3% BSA for 2 h. Protein samples were incubated with polyclonal antibody for 1 h at 37 °C. Monoclonal antibody MAB16988 (Chemicon, Temecula, CA) was used as primary antibody and horseradish peroxidase conjugated goat anti-murine IgG (Sigma, St Louis, MO) as secondary antibody. The reaction was performed with substrate (0.1mg/ml 3', 3', 5, 5'-tetramethylbenzidine in 50 mM citric acid, 0.003% H_2O_2) and stopped with 2 M H_2SO_4. The absorbance was determined at 450 nm with iMark Microplate Reader (Bio-Rad, Hercules, CA).

3.6. Western Blotting

To detect whether EA had an effect on HBV dimer or core protein, reducing SDS-PAGE (loading buffer containing 50 mM dithiothreitol and 1% SDS) and nonreducing SDS-PAGE (only 1% SDS, no dithiothreitol) were performed respectively. After disassembly reaction, samples were mixed with different loading buffers and boiled at 100 °C for 5 min followed by separation on 12% SDS polyacrylamide gel. Proteins were transferred onto PVDF (Pall, NY) and analyzed by immunoblotting with the polyclonal anti-HBc Ab.

3.7. Docking Analysis

Molecular formula of EA (NCBI PubChem Compound, CID 5281855) and structure of HBV capsid (Cp149) (Protein Data Bank code 1QGT) were prepared in order to predict the putative binding sites of EA and HBV capsid. In consideration of the fact that dimeric Cps assemble to capsid through a trimer of dimers [34], EA was blindly docked onto HBcAg monomer or hexamer using SwissDock server with default parameters.

4. Results

4.1. EA Causes HBV Mature Capsid Disassembly

To investigate the effect of EA on HBV capsid disassembly, native agarose gel analysis was used for detecting core particles (Figure 1B). With increasing concentrations of EA (25 to 250 μg/ml), disassembly of core particles increased progressively, whereas in the absence of EA, capsids remained intact. We further confirmed the disassembly of capsid by examining the morphological changes of disassem-

bled HBV capsids under EA treatment using TEM. In the presence of EA, core particles were aggregated together and showed detectable morphological alterations. Higher EA concentrations resulted in capsids depletion partially or totally. Meantime, the number of capsid particles also decreased drastically (Figure 1C). Thus, the TEM data further confirm the EA induces disassembly of core particles observed by agarose gel analysis.

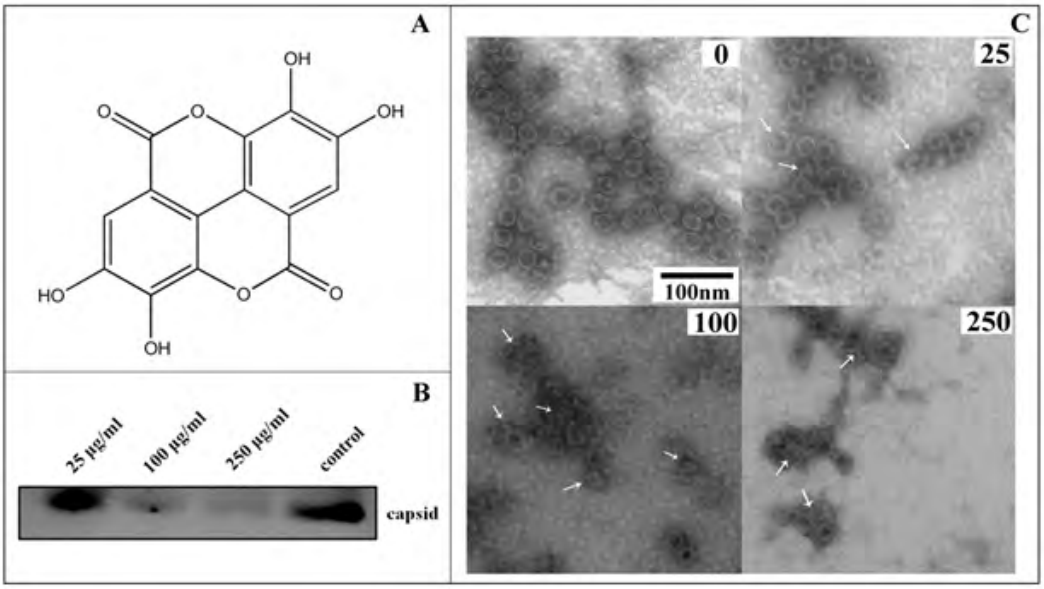

Figure 1: EA Causes HBV Capsid Disassembly.

(A) Structure of EA. (B) Core particles detected by native agarose gel electrophoresis. Compared to untreated control, the banding pattern of capsid becomes weaker with increasing EA concentrations, indicating the partial loss of core particles in EA concentration of 25 and 100 μg/ml, as well as near-complete loss in 250 μg/ml EA. (C) TEM shows that results of disassembly reaction are affected by EA concentrations. In the presence of EA, core particles are aggregated to each other and have obviously detectable morphological alterations, such as partial deletion. At the same time, amount of capsids decreased drastically. Disassembly level became higher as the chemical concentration increased from 25 to 250 μg/ml. White arrows identify examples of disassembled core particles. All images were captured at same magnification (scale bar = 100 nm).

4.2. Products of Capsid Disassembly

We further examined the results of disassembly by SEC. At 25 μg/ml chemical concentration, we observed a major peak in 16-17 ml. With increasing concentrations of EA, proteins were assigned to a great quantity of 10.3-17 ml elution fractions, ranging in a wide molecular weight variation from dimer to monomer (Figure 2A). This indicates that more heterogeneous aggregates were dissociated from the capsid with increasing concentrations of EA. We further evaluated the disassembly reactions of the capsid with 250 μg/ml EA at increasing time frames (0 h, 3 h, 6 h, 9 h and 12 h). The peak area of small heterogeneous aggregates increased gradually with increasing time of treatment, indicating that the disassembly process reached equilibrium slowly (Figure 2B). To quantify the disassembly level, we defined depolymerization coefficient as the ratio of incremental peak area of small heterogeneous aggregates to the reduced peak area of capsid in the presence of EA. The level of disassembly escalated with increasing EA concentrations (columns 1 to 3, Fig 2C) and reaction times (columns 3 to 6, Figure 2C). Thus, capsid disassembly is both EA concentration and treatment time dependent. Monoclonal antibody MAB16988 (Chemicon, Temecula, CA) can recognize core particle in capsid conformation, so it is highly selective for capsid compared to dimer [17]. Chromatography of proteins was analyzed by ELISA using the capsid-specific monoclonal antibody. ELISA horseradish peroxidase signals sustained a strong signal in capsid zone (7 to 8.3 ml), but a weak signal in the heterogenous aggregate zone (10.3 to 17 ml) (Figure 2D). The observation that heterogeneous aggregates are recognized by the monoclonal antibody indicates that the proteins in aggregates have a dimer-like conformation rather than capsid-like antigenicity.

4.3. EA Blocks Complete Dissociation of Dimer to Core Monomer

In SEC experiment, disassembly peaks mainly occurred between dimer and monomer region (Figure 2A and B). Thus, we conjectured EA could only separate core particles to small heterogeneous aggregates, rather than smaller proteins. To determine whether EA had an effect on HBV dimers or core monomers, non-reducing SDS-PAGE and reducing SDS-PAGE were performed respectively. Although, cysteine residues of HBV capsid protein are not required for dimer formation, they are needed for dimer and capsid stability in SDS [35]. Capsid treated with SDS could disassemble to dimers, but after breakage of the disulfide linkages, the depolymerization products would be core monomers. Under reducing SDS-PAGE conditions, untreated control showed a band of monomer (approximately

16 kDa), whereas dimer could be hardly detected. However, in the presence of EA, monomers could be detected in the membrane, as well as the dimers (approximately 35 kDa). In addition, the monomer band became weaker with the higher concentration of EA (Figure 3A). These results indicate that EA blocks further dimer separation into monomers, in spite of the disruption of the disulfide linkages by the reductant. Analogously, we reached a similar conclusion after performing nonreducing SDS-PAGE. In untreated control, dimer band was extremely intense while monomer could be also detected, indicating that majority of core particles dissociated to dimers, while only a small percentage further separated to core proteins. Unlike untreated control, the band pattern of dimer became more intense as the EA concentration increased from 25 to 250 μg/ml, while monomer band became weaker in 25 μg/ml or 100 μg/ml EA. At 250 μg/ml EA concentration, the monomer band almost faded away (Figure 3B). These results further show that EA blocks complete dissociation of dimer to core protein and further support the detection of small heterogeneous aggregates which are separated between dimer to monomer region in SEC. Furthermore, no other protein bands can be detected except dimer and monomer, indicating that EA is unable to disrupt core monomer. Thus, the loss of core particle signal in (Figure 1B) is due to the loss of capsid architecture rather than core protein degradation. Therefore, EA likely acts as an HBV core particle disassembly effector.

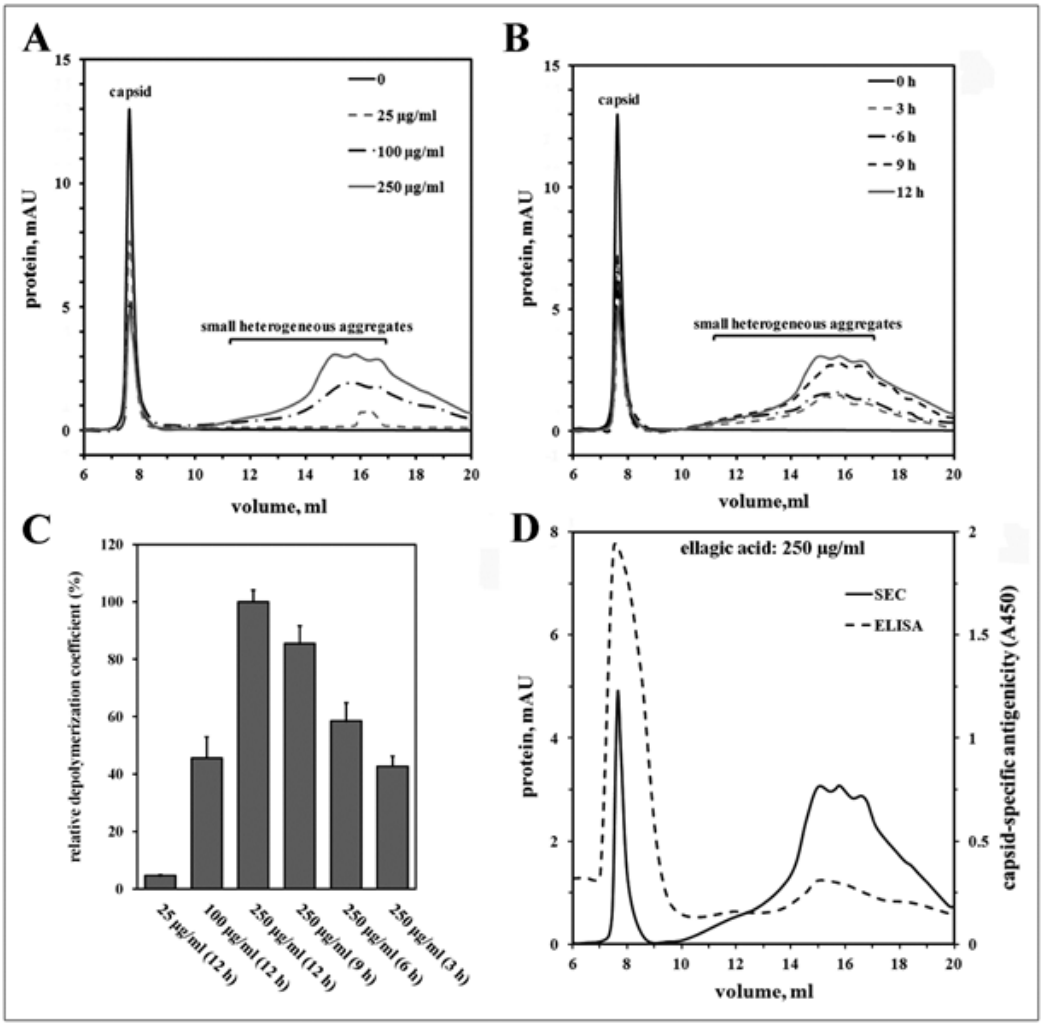

Figure 2: Capsid disassembly results in small heterogeneous aggregates which display dimer-like antigenicity.

(A) The size of the capsid peak eluted at approximately 7.0-8.3 ml was significantly reduced in the presence of EA. In 25μg/ml EA, a major peak is eluted at 16 to 17 ml. With increasing EA concentrations, a series of depolymerization peaks are eluted in a broad volume (10.3-17 ml), ranging in a wide molecular weight variation from dimer to monomer. (B) Time course dependent rate of disassembly reactions with 250 μg/ml EA at 0 h, 3 h, 6 h, 9 h and 12 h. The peak area of disassembly products increased gradually. (C) The disassembly level increased with increasing EA concentration or reaction time as shown by relative depolymerization coefficient values. (D) Disassembly reactions were performed with 250 μg/ml EA. Protein samples were detected by SEC (solid line). Fractions were collected and analyzed by ELISA using capsid-specific monoclonal antibody (dotted line). In the capsid zone, horseradish peroxidase signals were from 0.320 to 1.924. In the disassembly zone, ELISA signals were weakened drastically, ranging from 0.142 to 0.310.

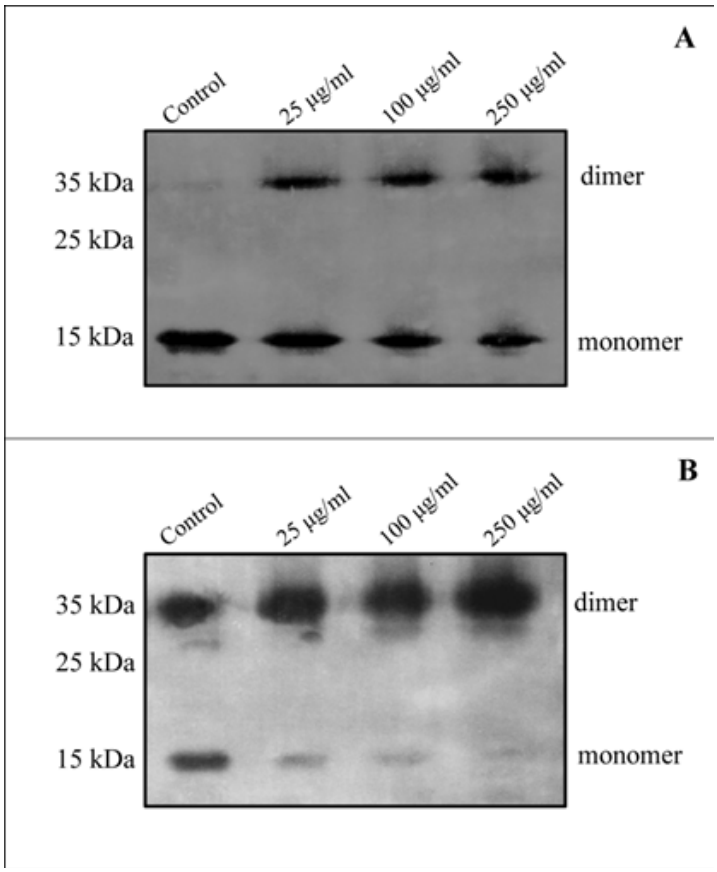

Figure 3: EA blocks dimer separation to core monomer.

(A) Under reducing SDS-PAGE conditions, untreated control only shows a band of monomer (16 kDa). In the presence of EA, both core protein and dimer (35 kDa) were detected. The monomer band became weaker with increasing concentration of EA from 25 to 250 μg/ml. (B) Under non-reducing SDS-PAGE conditions, dimer band was intense while monomer band was weaker in untreated control. The monomer band became weaker with increasing EA concentration and further faded in presence of 250 μg/ml EA.

4.4. Putative Capsid Binding Sites of EA

There is no unambiguous data to identify the site for EA binding to capsid. With SwissDock server, two possible binding sites were calculated in our study: (I) Docking EA onto HBcAg monomer revealed a binding site (Figure 4A) similar to that of the assembly effector HAP-1 [36], with the estimated interaction energy of −6.36 kcal/mol. Within a monomer, the putative interaction site was mainly linked with hydrophobic residues, including Thr33, Trp102, Ile105, Ser106, Tyr118 and Leu140. EA bound to Trp102 and Ser106 by a hydrogen bond (Figure 4B); (II) An alternative binding site was also revealed by docking EA onto HBcAg hexamer. The dimers in a hexamer, named AB, CD and EF, constituted two capsid-like interdimer contacts, B-C and D-E junctions, but no F-A contact [37]. The putative binding site settled at the interface of two assembly unit, i.e. D-E contact (Figure 4C), with the interaction energy of −6.38 kcal/mol. The putative interacting residues in chain D were Thr142 and Leu143, while Tyr118, Pro138, Ile139 (hydrogen bond) and Leu143 were feasible binding residues in chain E of another assembly unit (Figure 4D).

5. Discussion

The capsid structure is critical for the mature nucleocapsid. Our study demonstrates that the antiviral effect of EA is primarily due to the disassembly of capsid. EA disrupts core particles to disassemble into small heterogeneous aggregates, thereby destroying the intact HBV virus particle and block the normal function of virus particle in the life cycle of HBV.

EA disrupted the capsid and promoted the disassembly of capsid in dose-dependent manner. With increasing EA concentrations, more heterogeneous aggregates were released from the capsid (Figure 2A). Large-scale disassembly required considerably higher EA concentrations. In addition, the disassembly rate remained similar between 0 to 12 hrs when capsids were treated with EA (Figure 2B). The ratio of capsids to small heterogeneous aggregates became higher with the prolonged treatment of capsids with EA (Figure 2C), indicating that capsid disassembly was a time consuming procedure rather than an instantaneous one.

The docking analysis showed EA bound to residues Trp102, Ile105 and Ser106 in site I (Fig.4B), which might affect dimer equilibrium, based on the fact that amino acids 78-117 forms part of the dimer interface [38]. Residues Glu113 to Leu143 mainly contributed to dimer multimerization [38,39]. Binding to residues Pro138 and Ile139 in site II (Figure 4D) likely outweighed the inter-subunit interaction

between amino acids 128-139 [21,40] and the binding energy was also sufficient to break the weak protein-protein interactions [41]. Consequently, some disassembly aggregates were separated from core particles. The ELISA results further supported that disassembly products were small heterogeneous aggregates which carried negligible levels of capsid-specific antigen epitope (Figure 2D). EA mainly bound to site I and II (Fig. 4) of mature capsid, which might alter the conformation of either monomer or dimer sufficiently, resulting in the formation of the small heterogeneous aggregates. This further blocked complete dimer separation to core monomers even in the presence of strong reductant, leading to accumulation of more dimeric proteins at higher EA concentrations (Figure 3). This supported the results that disassembly peaks were mainly separated between dimer and monomer region in SEC (Figure 2). Thus EA as a drug penetrates into the capsid in specific sites to induce the metastable capsid, resulting in capsid disassociation to small heterogeneous aggregates. Further research on EA analogs with higher interaction energy may lead to the development of more effective therapies against HBV infections.

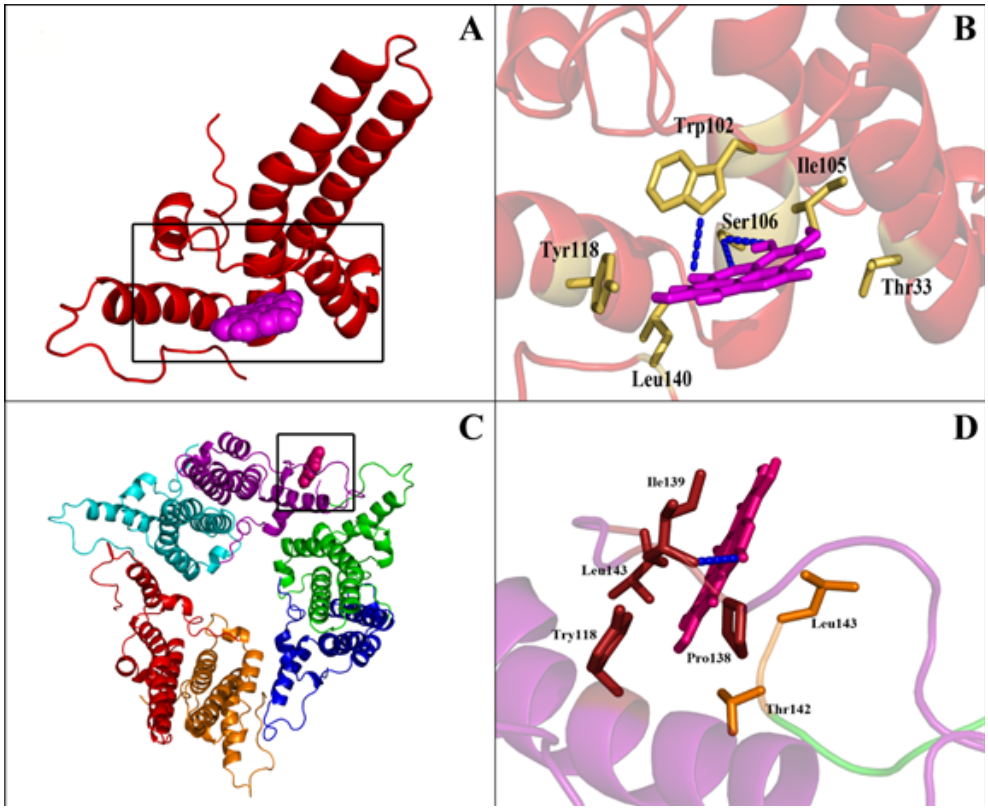

Figure 4: Docking analysis identifies two putative binding sites.

(A) The putative EA interacting site is located in a similar cavity associated with a monomer (red) (as previously observed with HAP-1). EA molecule is identified by hot pink sphere. (B) Close up of the site shown boxed in (A). EA links with the hydrophobic residues Thr33, Trp102, Ile105, Ser106, Tyr118 and Leu140. EA binds to Trp102 and Ser106 by a hydrogen bond (blue dotted line). (C) The alternative binding site is shown in an HBcAg hexamer. EA molecule (hot pink) links the D-E contact in the hexamer. Chain A, B, C, D, E, and F are colored by red, orange, blue, green, purple, and cyan, respectively. (D) Close up of the site shown boxed in (C). The binding site is comprised of Thr142 and Leu143 from chain D and Tyr118, Pro138, Ile139 and Leu143 from chain E. The hydrogen bond between EA and Ile139 is marked with blue dotted line.

6. Conflict of Interest Statement

The authors declare that they have no known competing financial interests or personal relationships that could influence the studies described in this article.

7. Authors' Contributions

Q.H. Liu conceived and designed the experiments; P. Wang, H. Sun and Q.H. Liu performed the experiments, analyzed the data and wrote the manuscript. All authors read and approved the manuscript in its finalized form.

8. Data Availability Statement

The datasets generated during and/or analysed during the current study are available from the corresponding author on reasonable request.

9. Acknowledgement

This study was supported by a grant from the National Key R&D Program of China (Project No. 2018Yfd04000200) and China Agriculture Research System (No. CARS-20-08B).

References

1. Wiersma ST, McMahon B, Pawlotsky JM, Thio CL, Thursz M, Lim SG, et al. Treatment of chronic hepatitis B virus infection in resource-constrained settings: expert panel consensus, Liver Int. 2011; 31: 755-761.
2. Lai CL, Ratziu V, Yuen MF, Poynard T, Viral Hepatitis B. Lancet. 2003; 362: 2089-2094.
3. Blumberg BS, London WT. Hepatitis B virus: pathogenesis and prevention of primary-cancer of the liver, Cancer. 1982; 50: 2657-2665.
4. London WT, Blumberg BS. A cellular-model of the role of hepatitis B virus in the pathogenesis of primary hepatocellular-carcinoma. Hepatology. 1982; 2: S10-S14.
5. Lesmana LA, Leung NWY, Mahachai V, Phiet PH, Suh DJ, Yao G, et al. Hepatitis B: overview of the burden of disease in the Asia-Pacific region, Liver Int. 2006; 26: 3-10.
6. Karayiannis P. Current therapies for chronic hepatitis B virus infection, Expert rev. anti-infe. 2004; 2: 745-760.
7. Wands JR. Prevention of hepatocellular carcinoma. N Engl J Med. 2004; 351: 1567-1570.
8. Lok AS. Hepatitis B infection: pathogenesis and management. J. Hepatol. 2000; 32: 89-97.
9. Cuestas ML, Mathet VL, Oubiña JR, Sosnik A. Drug delivery systems and liver targeting for the improved pharmacotherapy of the hepatitis B virus (HBV) infection. Pharm. Res. 2010; 27: 1184-1202.
10. Delaney WE, Yang H, Westland CE, Das K, Arnold E, Gibbs CS, et al. The hepatitis B virus polymerase mutation rtV173L is selected during lamivudine therapy and enhances viral replication in vitro. J. Virol. 2003; 77: 11833-11841.
11. Jardi R, Rodriguez-Frias F, Schaper M, Ruiz G, Elefsiniotis I, Esteban R, et al. Hepatitis B virus polymerase variants associated with entecavir drug resistance in treatment-naive patients. J. Viral Hepatitis. 2007; 14: 835-840.
12. Ayoub WS, Keeffe EB. Review article: current antiviral therapy of chronic hepatitis B, Aliment. Pharmacol. Ther. 2011; 34: 1145-1158.
13. Seeger C, Mason WS. Hepatitis B virus biology, Microbiol. Mol. Biol. Rev. 2000; 64: 51-68.
14. Zlotnick A, Stray SJ. How does your virus grow? Understanding and interfering with virus assembly. Trends Biotechnol. 2003; 21: 536-542.
15. Stannard LM, Hodgkiss M. Morphological irregularities in dane particle cores. J. Gen. Virol. 1979; 45: 509-514.
16. Crowther RA, Kiselev NA, Böttcher B, Berriman JA, Borisova GP, Ose V, et al. P. Three-dimensional structure of hepatitis B virus core particles determined by electron cryomicroscopy. Cell. 1994;; 77: 943-950.
17. Stray SJ, Ceres P, Zlotnick A. Zinc ions trigger conformational change and oligomerization of hepatitis B virus capsid protein. Biochemistry. 2004; 43: 9989-9998.
18. Wingfield PT, Stahl SJ, Williams RW, Steven AC. Hepatitis core antigen produced in Escherichia coli: subunit composition, conformational analysis, and in vitro capsid assembly. Biochemistry. 1995; 34(15): 4919-4932.
19. Choi Y, Gyoo Park S, Yoo JH, Jung G. Calcium ions affect the hepatitis B virus core assembly. Virology. 2005; 332: 454-463.
20. Uetrecht C, Versluis C, Watts NR, Roos WH, Wuite GJL, Wingfield PT, et al. High-resolution mass spectrometry of viral assemblies: Molecular composition and stability of dimorphic hepatitis B virus capsids. Proc. Natl. Acad. Sci. USA. 2008; 105: 9216-9220.
21. Wynne SA, Crowther RA, Leslie AGW. The crystal structure of the human hepatitis B virus capsid. Mol. Cell. 1999; 3: 771-780.
22. Zlotnick A, Ceres P, Singh S, Johnson JM. A small molecule inhibits and misdirects assembly of hepatitis B virus capsids. J. Virol. 2002; 76: 4848-4854.
23. Deres K, Schröder CH, Paessens A, Goldmann S, Hacker HJ, Weber O, et al. Inhibition of hepatitis B virus replication by drug-induced depletion of nucleocapsids. Science. 2003; 299: 893-896.
24. Stray SJ, Zlotnick A. BAY 41-4109 has multiple effects on hepatitis B virus capsid assembly. J. Mol. Recognit. 2006; 19: 542-548.
25. Stray SJ, Bourne CR, Punna S, Lewis WG, Finn MG, Zlotnick A, et al. A heteroaryldihydropyrimidine activates and can misdirect hepatitis B virus capsid assembly, Proc. Natl. Acad. Sci. USA. 2005; 102(23): 8138-8143.
26. Venkateswaran PS, Millman I, Blumberg BS. Effects of an extract from Phyllanthus niruri on hepatitis B and woodchuck hepatitis viruses: In vitro and in vivo studies. Proc. Natl. Acad. Sci. USA. 1987; 84(1): 274-278.
27. Yeh SF, Hong CY, Huang YL, Liu TY, Choo KB, Chou CK, et al. Effect of an extract from Phyllanthus amarus on hepatitis B surface antigen gene expression in human hepatoma cells, Antiviral Res. 1993; 20(3): 185-192.
28. Lee CD, Ott M, Thyagarajan SP, Shafritz DA, Burk RD, Gupta S. Phyllanthus amarus down-regulates hepatitis B virus mRNA transcription and replication. Eur. J. Clin. Invest. 1996; 26: 1069-1076.
29. Shin M, Kang E, Lee Y. A flavonoid from medicinal plants blocks hepatitis B virus-e antigen secretion in HBV-infected hepatocytes, Antiviral Res. 2005; 67(3): 163-168.
30. Girish C, Pradhan SC. Drug development for liver diseases: focus on picroliv, ellagic acid and curcumin. Fund. Clin. Pharmacol. 2008; 22(6): 623-632.
31. Kang EH, Kown TY, Oh GT, Park WF, Park SI, Park SK, et al. The flavonoid ellagic acid from a medicinal herb inhibits host immune tolerance induced by the hepatitis B virus-e antigen, Antiviral Res. 2006; 72(2): 100-106.
32. Zlotnick A, Cheng N, Conway JF, Booy FP, Steven AC, Stahl SJ, et al. Dimorphism of hepatitis B virus capsids is strongly influenced by the C-terminus of the capsid protein. Biochemistry. 1996; 35(23): 7412-7421.
33. Park SG. Antisense oligodeoxynucleotides targeted against molecular chaperonin hsp60 block human hepatitis B virus replication. J. Biol. Chem. 2003; 278(41): 39851-39857.
34. Zlotnick A, Johnson JM, Wingfield PW, Stahl SJ, Endres D. A theoretical model successfully identifies features of hepatitis B virus capsid assembly. Biochemistry. 38(44): 14644-14652.

35. Zhou S, Standring DN. Cys residues of the hepatitis B virus capsid protein are not essential for the assembly of viral core particles but can influence their stability. J. Virol. 1992; 66(9): 5393-5398.

36. Bourne CR, Finn MG, Zlotnick A. Global structural changes in hepatitis B virus capsids induced by the assembly effector HAP1. J. Virol. 2006; 80(22): 11055-11061.

37. Packianathan C, Katen SP, Dann CE, Zlotnick A. Conformational changes in the hepatitis B virus core protein are consistent with a role for allostery in virus assembly. J. Virol. 2009; 84(3): 1607-1615.

38. Konig S, Beterams G, Nassal M. Mapping of homologous interaction sites in the hepatitis B virus core protein. J. Virol. 1998; 72(6): 4997-5005.

39. Newman M, Chua PK, Tang FM, Su PY, Shih C. Testing an electrostatic interaction hypothesis of hepatitis B virus capsid stability by using an in vitro capsid disassembly/reassembly system. J. Virol. 2009; 83(20): 10616-10626.

40. Steven AC, Conway JF, Cheng N, Watts NR, Belnap DM, Harris A, et al. Structure, Assembly, and Antigenicity of Hepatitis B Virus Capsid Proteins, Adv. Virus Res. 2005; 64: 125-164.

41. Ceres P, Zlotnick A. Weak protein-protein interactions are sufficient to drive assembly of hepatitis B virus capsids, Biochemistry. 2002; 41(39): 11525-11531.